# Reverse Monte Carlo Modeling of Radiative Transfer in a Clumpy Molecular Cloud

Ryan Armstrong, Maggie Hilderbran, Samantha Pagan

Final Report

Report Submitted: November 28, 2017

PHYS 358

# 1 Introduction

Molecular clouds are interstellar clouds of size and density capable of forming molecules [4] (Larson). Observations show the molecules are not evenly distributed throughout the cloud's structure [1]. The high density "clumps" are the beginning of star formation (Larson). The chemical reaction rates driving the stellar development are dependent on the ambient radiation field. Therefore, an understanding of radiation within molecular clouds is important to understanding stellar evolution. Our project will investigate the radiation field by first modeling a structured molecular cloud and then preforming a reverse Monte-Carlo procedure to quantify the propagation of radiation from changing views and density contrasts.

# 2 Background and Theory

Radiative transfer is an approximate model of light propagation. The method assumes that (1) light propagates geometrically as a ray and (2) that the index of refraction $n$ is uniform. Thus, photons travel in straight lines as rays of light until they are impacted by a scattering event that changes their path. Additionally, photons may be created or absorbed [2, p. 3]. This model for radiative transfer simplifies the matter of radiation propagation into something that can be modeled simply.

In this project, we consider the propagation of radiation in a molecular cloud. To model radiative transfer inside the cloud, it is necessary to understand how the trajectory of a photon is continually altered by scattering events. A photon will proceed a certain distance until being scattered in a new direction, then move forward until the next scattering event.

Optical depth, denoted by $\tau$, provides information about the average number of scatterings along a photon's path. A high optical depth ($\tau >> 1$) means one would expect a high number of scatterings, and a low optical depth ($\tau << 1$) corresponds with very few scatterings on average. While optical depth can be considered a characteristic of a certain distance, $\tau$ is unitless and not a length itself.

To assess the optical depth a photon will reach before being scattered, a probabilistic approach is used. The probability $p$ of a photon reaching an optical depth $\tau_s$ before scattering is given by

$$p = \exp(-\tau_s). \tag{1}$$

Equation (1) is at the core of radiation propagation models and will be addressed in Section 3.2.2.

# 3 Methods

To implement our modeling of radiative transfer by Monte Carlo methods, we must have methods for (1) constructing a simulated medium through which photons can travel and (2) modeling the movement of photons in this medium. For the former, we can utilize test cloud creation mechanisms developed in Mathis et al. 2002 [5]; for the latter, we can implement the reverse Monte Carlo method used by Bethell et al. 2004 [1].

## 3.1 Modeling the Cloud

### 3.1.1 Procedure from Mathis et al. 2002

Uniform clouds are inherently easier to model. However, radiation transfer differs between uniform and non-uniform media. For example, a photon will travel more freely in the low-partial regions between clumps of a non-uniform cloud than in a uniform cloud of the same mass and volume. Therefore, to most accurately describe the radiation in molecular clouds (which are known to be structured), a structured model must be used [5].

The density structure of molecular clouds is said to be self-similar on all size scales. To attempt to replicate this, our model is hierarchical. This means it will be self-similar on a finite scale [5].

1. Establish a "supercube" of length $L$. The cube is deemed a supercube because it is made from stacked sub-cubes.

2. Randomly place $N$ points within the supercube. Mathis et al. set $N = 32$.

3. Determine a desired fractal dimension, $D$, which defines the density of the supercube's self-similar nature (i.e. how closely in space the density structure repeats). The degree of clumping of observed molecular clouds falls within the range $2.3 < D < 2.6$ [5, p. 813]

4. Define a sphere of radius $L/(2\Delta)$ around each of the $N$ random points from step (2). The value $\Delta$ satisfies the equation $D = log(N)/log(\Delta)$.

5. Randomly place $N$ points within the N spheres defined in step (4). Allow for points to fall outside the supercube.

6. Repeat steps (4) and (5) twice more to bring the total number of points to $N^4$. The self-similar nature of the distribution should now be clear.

7. Define external coordinates as Cartesian coordinates with magnitude greater than $L/2$. Points containing external coordinates fall outside the supercube. Reflect any points exterior of the supercube into the supercube by shifting the external coordinates towards the origin by $L$. At this point, all points are contained within the supercube. The density of the supercube is therefore proportional to the number of points within each cell.

8. Inscribe a sphere within the supercube. In Mathis et al., a source of radiation was placed at the origin. However, for our project, photons enter the molecular cloud from the exterior. Therefore, the source is omitted. Finally, a constant of proportionality is used to relate the density of the model to the desired mean optical depth $\tau_0$.

The sphere within the supercube now represents a four-tier hierarchically structured clumped molecular cloud. If desired, a uniform set of points could be added to each cell as observed molecular clouds do not have volumes of complete emptiness. The model of the molecular cloud is now ready to have numerical simulations performed on it [5].

## 3.2 Modeling Radiative Transfer

### 3.2.1 Reverse Monte Carlo

Monte Carlo methods are used when analytic solutions are difficult or impossible to obtain [6]. Because of the many variables, unknowns, and uncertainties of molecular clouds, an analytical solution is not feasible for studying radiative transfer. For this project a reverse Monte Carlo method will be used to model photons propagating through a cloud. Using a reverse Monte Carlo method increases computational efficiency, and based on previous traditional forward Monte Carlo methods of clouds this is still an effective modeling scheme [1].

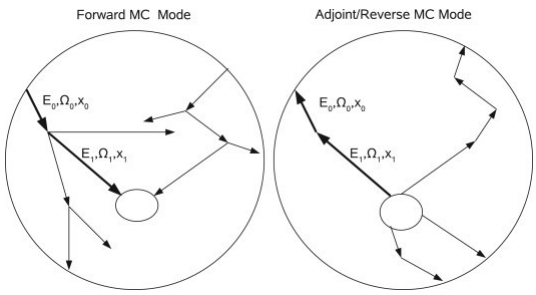


Figure 1: A representation of reverse Monte Carlo (https://ars.els-cdn.com/content/image/1-s2.0-S0168900210011836-gr1.jpg)

### 3.2.2 Implementation (Bethell et al. 2004)

To model propagation of radiation, a reverse Monte Carlo approach can be adopted in which photon paths are traced outwards from the point of observation. The method described in this subsection is paraphrased from Bethell et al. 2004 [1].

First, one can obtain a random value $\tau_s$ from the distribution given by Equation (1) in Section 2. The function for $p$ can be inverted to obtain

$$\tau_s = -\ln(p), \tag{2}$$

where $p$ is sampled from a uniform distribution across an interval [0,1]. Random values of $p$ can be used to calculate corresponding values of $\tau_s$, modeling a photon's propagation along some path.

This optical depth $\tau_s$ can be converted to an actual path length $l$ for the photon. The optical depth $\tau_s'$ of some path can be calculated by

$$\tau_s' = \sum \sigma_s(\lambda) n_H \Delta l, \tag{3}$$

where $\sigma_s(\lambda)$ is the scattering cross-section and $n_H$ is the number density of the cloud molecules. We can calculate $\tau_s'$ with successive iterations of $\Delta l$ until $\tau_s'$ is close enough to $\tau_s$ within a specified margin of error. The sum of the steps $\Delta l$ yields a total physical length $l$ in space.

After the photon is advanced by $l$, the scattering event must be modeled. We can use the Henyey-Greenstein phase function [3] used by Bethell et al. 2004:

$$\Phi(\theta) = \frac{(1/4\pi)(1-g^2)}{(1+g^2-2g\cos\theta)^{3/2}}, \tag{4}$$

where $g$ is the asymmetry parameter ($-1 \leq g \leq 1$). Using Equation (4), the deflection angle $\theta(p)$ can be calculated as a function of $p$, a random, uniformly distributed number between 0 and 1 as

$$\theta(p) = \frac{(1+g^2) - [(1-g^2)/(1-g+2gp)]^2}{2g}. \tag{5}$$

The azimuthal deflection angle $\phi$ is obtained more simply:

$$\phi = 2\pi p, \tag{6}$$

where p is (once again) a uniformly distributed, random number between 0 and 1.

The set of calculated angles ($\theta$,$\phi$) yields a new direction for the scattered photon. Scatterings can then be repeatedly modeled until the photon reaches the cloud's surface.

We can assess the intensity of radiation at a point $\mathbf{A}$ in the cloud when observing along a direction $\hat{\mathbf{k}}_{\mathbf{obs}}$ as done in Bethell et al. 2004. For a given direction $\hat{\mathbf{k}}_{\mathbf{obs}}$, we can calculate $M$ different trajectories of photon scattering. Then, we can repeat this process for $N$ different directions $\hat{\mathbf{k}}_{\mathbf{obs}}$. The equation for the mean relative intensity is:

$$\frac{J(\mathbf{A})}{I_0} = \frac{1}{N}\sum_n^N \frac{I(\hat{\mathbf{k}}_{\mathbf{obs}}, \mathbf{A})}{I_0} = \frac{1}{NM}\sum_n^N \sum_m^M W_{nm}, \tag{7}$$

where $W_{nm}$ values are the weights given by

$$W = \exp(-\tau_a^{tot}) \tag{8}$$

and $\tau_a^{tot}$, the total optical absorption depth of the photon's path, is

$$\tau_a^{tot} = \sum (\omega^{-1} - 1)\tau_s, \tag{9}$$

where $\omega$ is the albedo. Thus, we can use Equation (7) to obtain a value for the total mean relative intensity at the point $\mathbf{A}$.

# 4 Results

## 4.1 Representation of Data

As stated in the methods, the code produces the intensity values at points throughout the molecular cloud. The intensity data can be displayed by plotting two dimensional slices of the cloud (with intensity values color-mapped) as well as plotting average intensities against radius.

## 4.2 Standard Cloud

The simulation of the molecular cloud and radiative transfer took parameters for albedo ($\omega$), mean radial optical depth ($\tau_0$), fractal dimension ($D$), number of observation directions ($N$), number of trajectories ($M$), and the length of the supercube ($L$). To view the effects of altering these parameters, a 'standard' cloud and simulation was created. An identical cloud was created for each simulation by seeding the random number generators. Specifically, the 'standard cloud' used was seeded with *random.seed(4)*. Additionally, the 'standard cloud' had an albedo of 0.5, mean optical depth of 2.0, fractal dimension of 2.3, and supercube length of 64. The standard was run with 10 directions, 5 trajectories, and 100,000 observation points. As will be discussed later, the cloud would have been ideally run with $N \approx L^2$ and $M \approx 10$. These values were not used for time constraints. The described standard cloud takes $\approx 25$ minutes to run. Because $N$ and $M$ have linear time complexities, using the ideal values would multiply the run time by $(64^2/10)(10/5) = 819$, yielding a run of 14 days. We believed the standard cloud was the balance between having enough time to run all the tests and producing enough results to see patterns. A slice of the standard cloud and its intensity versus radius graph are shown on the bottom half of Figure[2]. Additionally, the top of Figure[2] is the 'most accurate' version of the cloud we could create given computing resources. The cloud on top used $N = 100$ and $M = 10$ and ran fro 8.5 hours. As seen, their results are similar, suggesting the standard cloud is a reasonable test cloud.

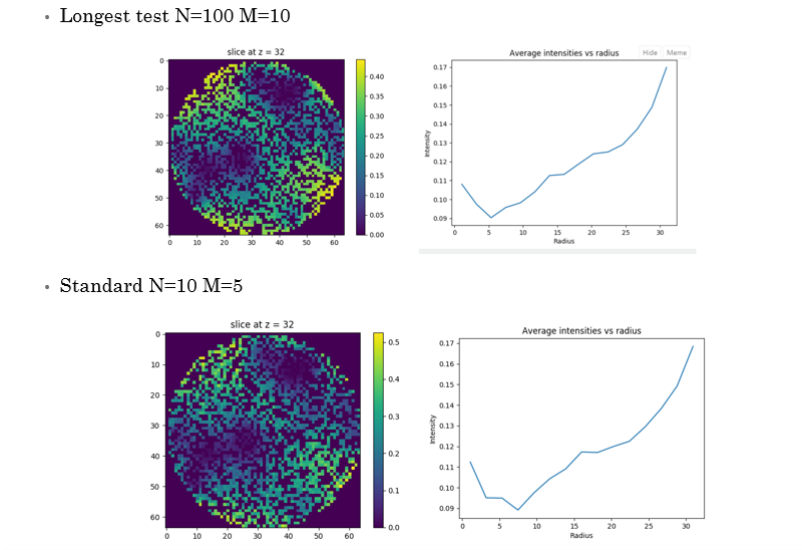


Figure 2: Similarity between our 'best' (top) and 'standard' (bottom) clouds and simulations

## 4.3 Effects of Cloud Parameters

The standard cloud was used to test the effects of the albedo, mean radial optical depth, fractal dimension, and length of the supercube. While holding all other parameters constant, each parameter was changed to a value above and below the value it is in the standard cloud. These variations are obvious through slice data alone, therefore, the intensity versus radius plots will not be shown.

### 4.3.1 Albedo

The albedo is a grain property that describes the "fraction of the extinction that is scattering" [5, p. 812]. Therefore, a lower albedo absorbs a higher proportion of light. As shown from the cross sections in Figure [2] below, the clouds with higher albedo have higher intensity because less light is absorbed.

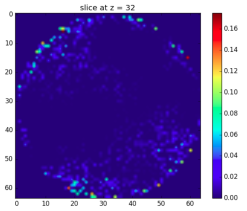


(a) A cloud with albedo of 0.1

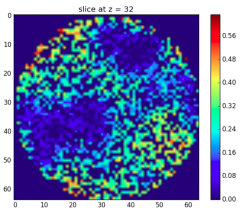


(b) A cloud with albedo of 0.5

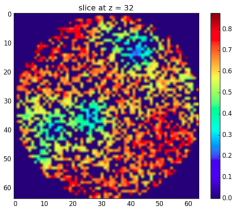


(c) A cloud with albedo of 0.8

Figure 3: Intensity slices for clouds of varying albedos

#### 4.3.2 Mean Radial Optical Depth

Changing the optical depth $\tau_0$ produced results that aligned with our expectations. With a higher optical depth, the intensity was uniformly lower across the cloud; with a lower optical depth, the intensity was higher. Additionally, we expected higher optical depths to correspond with longer run times because photons would require more scatterings to escape clouds with higher optical depths. The results matched this expectation as well. The intensities can be seen in Figure [3] below. Additionally, the run time of $\tau_0 = 0.1$ was 68 sec, $\tau_0 = 2$ was 297 sec, and $\tau_0 = 10$ was 1697 sec.

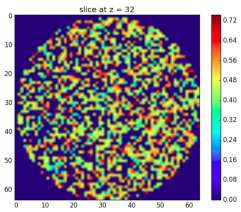


(a) A cloud with optical depth of 0.1

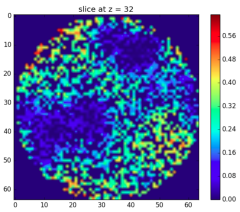


(b) A cloud with optical depth of 2

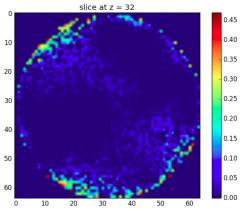


(c) A cloud having optical depth of 10

Figure 4: Intensity slices for clouds of varying optical depths

#### 4.3.3 Fractal Dimension

Changing the fractal dimension is supposed to change the degree of clumping within the cloud. A value of 2.3 - 2.6 was recommended. [5, p. 813]. The fractal dimension was tested at $D = 1.5, 2.3, 3.0$. The slices are shown in Figure[4]. While the clouds are clearly different, it is difficult to describe the effect of the fractal dimension. More tests (with different clouds and more slicing) would have to be conducted to draw a conclusion.

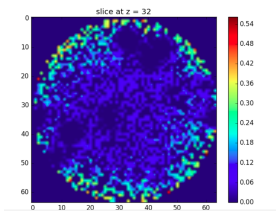


(a) A cloud with $D = 1.5$

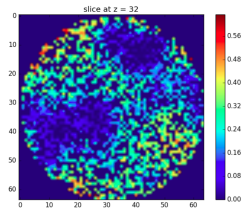


(b) A cloud with $D = 2.3$

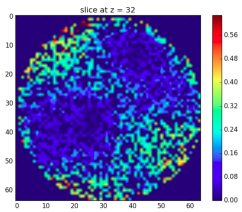


(c) A cloud with $D = 3.0$

Figure 5: Intensity slices for clouds of varying fractal dimensions

#### 4.3.4 Length of the Supercube

The length of the supercube determines the resolution of the intensity solution. Therefore, increasing the length of the supercube should have a generally positive impact on the model. However, as seen by Figure [5], increasing the supercube without increasing the number of observation points creates an cloud that is too sparse to draw conclusions. Because the volume of the cube increases by $\delta L^3$, a doubling of the length would require $A^3$ observation points to fill the cube as densely as previously.

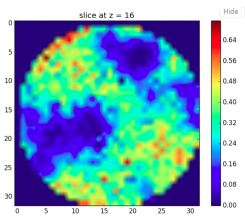


(a) 32 supercubes per dimension

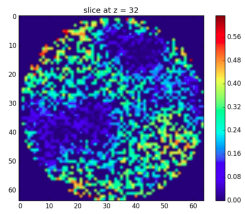


(b) 64 supercubes per dimension

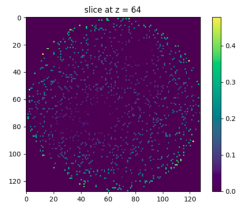


(c) 128 super cubes per dimension

Figure 6: Intensity slices for clouds with varying numbers of subcubes

## 4.4 Effects of Simulation Parameters

## 4.5 Varying N

$N$ represents the number of direction of observation. The parameter $N$ was varied to be 1, 10, and 100. As stated, the ideal number of observations would be $N \approx L^2$. Using the ideal will ensure all array values are sampled. However, run time does not allow this ideal. Nevertheless, as $N$ was increased the overall intensity scale in each graph decreased, and it can be concluded that the maximum intensity decreased. This is most likely due to higher sampling making it less probably

for the photon to pass through the cloud without interacting with a clump.

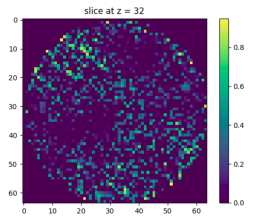


(a) N=1

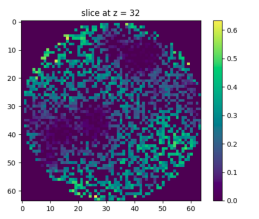


(b) N=10

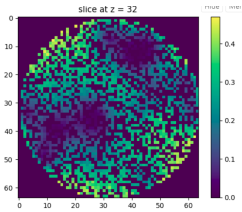


(c) N=100

Figure 7: Varying N

## 4.6 Varying M

$M$ represents the number of trajectories. The parameter $M$ was also varied to be 1, 10, and 100. similar to $N$, as $M$ was increased the overall scale also decreased. The number of trajectories also increases sampling similarly making it less probably for the photon to pass through the cloud without interacting with a clump.

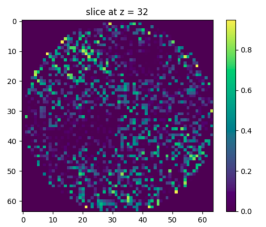


(a) M=1

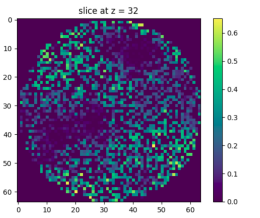


(b) M=10

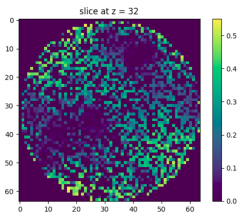


(c) M=100

Figure 8: Varying M

## 4.7 Types of Test Clouds

The clumpy cloud was then compared to a uniform cloud and a cloud or a structured hierarchy (where the density of points is forced to decrease as radius increases). This clouds are visualized in Figures [6-8].

The intensity versus radius graphs for the three clouds were produced. These plots are shown in Figure[9]. As expected, all clouds have the lowest intensity at the center of the cloud. However, from both the slices and the graph shapes, the clumpy graph showed higher intensity at the center

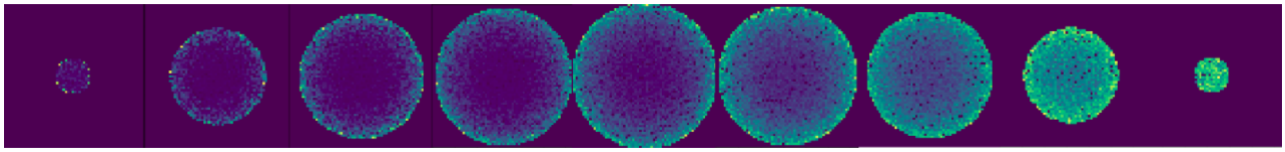

Figure 9: Slices of a Uniform Cloud

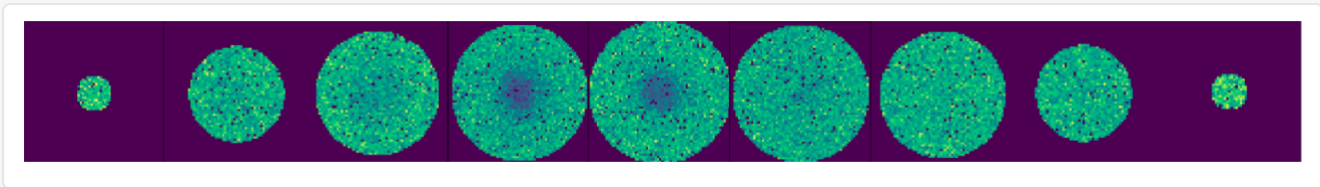

Figure 10: Slices of a hierarchal cloud

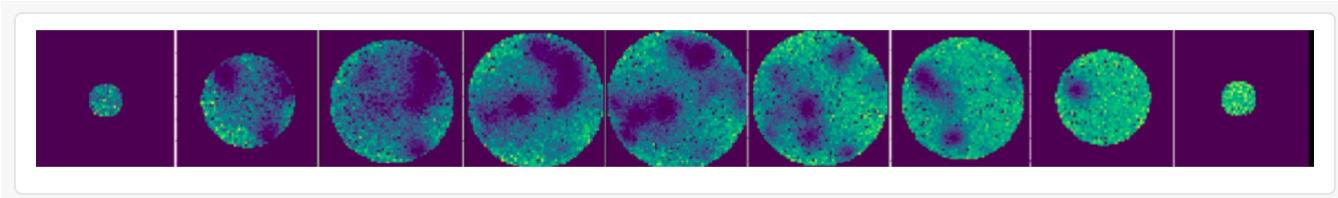

Figure 11: Slices of Clumpy Clouds

and more variability in the intensity at any radii. This is a vital observation to make. Many chemical reactions within a molecular cloud require minimum amount of UV light. If chemical reaction rates are determined using a uniform or hierarchical cloud, these rates will be lower compared to a clumpy model, which–as stated previously–are the observed clouds. It should also be noted by the slices that the clumpy model has a much higher average intensity than the uniform model (as they both have the same average optical depth, but much more of the clumpy clouds space is sparse). Therefore, reaction rates would be quicker across most of the cloud (i.e. the non clumped regions). This would have been observed in the hierarchical structure as well, however the center was so dense that it appeared as clump.

# 5 Challenges and Features Added

## 5.1 Run Time

Run time was the largest challenged faced. Building the cloud has a time complexity of O($N^4$), finding mean intensities has a time complexity of O($MN$), sampling $A$ observation points has a time complexity of O($A$) and determining any path-length has an approximate worst case time complexity of O($L$). Therefore, as the code is currently implemented, the overall worst case time complexity for a solution is O($ANML + N^4 Res^2 L$). This is the result of looping $A$ times (for $A$ points), each with $N$ observational directions and $M$ trajectories which carry path-length calculations $L$ all after creating a cloud of $N^4$ points, determining its mean optical depth by taking path lengths, $L$, for a $Res^2$ number of trajectories. Clearly, the code relies on large iterations. This is partially due to the three-dimensional nature and partially due to Monte-Carlo schemes relying on random numbers (and therefore heavy sampling). To combat this, we ran small numbers of iterations and created printouts that would use *timeit* measures in the loops to estimate total runtime. Perhaps a different language or techniques like using Numba to compile pieces of the code could have helped this problem and could be suggested to future groups.

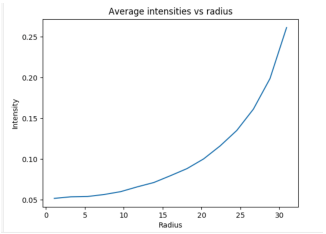


(a) Uniform cloud

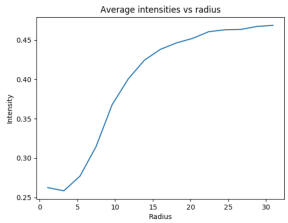


(b) Hierarchical cloud

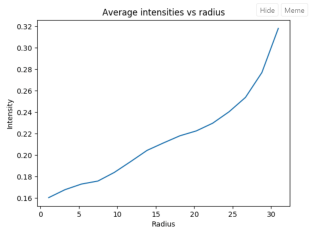


(c) Clumpy Graph

Figure 12: Intensity vs radius for the uniform, structured, and clumpy clouds

### 5.2 Testing with Different Types of Clouds

Because our two main parts of our project were to create a cloud and then run through the reverse Monte Carlo, it was challenging to test the results of Monte Carlo without complete confidence of a correct cloud. To attempt to test the radiative transfer modeling of our project we also ran our code with a uniform density cloud. When versions of our code showed no difference between our uniform cloud and a modeled clumpy cloud, it was a large indication of what aspects of our code were creating problems and a helpful tool for debugging.

## 6 Conclusion

In this project, we modeled the propagation of EM radiation through a structured molecular cloud by using a reverse Monte Carlo method. Our clouds were created using a procedure developed by Mathis et al. 2002 [5], and the reverse Monte Carlo method came from Bethell et al. 2004 [1]. We then created a model cloud and varied our simulation parameters for that particular cloud to see the effects of changing the albedo, the mean radial optical depth, the fractal dimension, and the number of subcubes per supercube side. We also compared the results of our hierarchical test cloud to a cloud with a uniform density and one with a pre-determined density proportional to the distance from the center. Though our code successfully modeled these scenarios, one of our largest challenges was long run times when we ran our simulations. Future work could include efforts to speed up the code and run more simulations.

## References


[1] Thomas J. Bethell, Ellen G. Zweibel, Fabian Heitsch, and J. S. Mathis. Dust heating in turbulent molecular cloud models. *The Astrophysical Journal*, 610(2):801–812, August 2004.

[2] C.P. Dullemond. Radiative transfer in astrophysics: Lecture notes. http://www.ita.uni-heidelberg.de/~dullemond/lectures/radtrans_2012/.

[3] L. G. Henyey and J. L. Greenstein. Diffuse radiation in the galaxy. *The Astrophysical Journal*, 93:70–83, January 1941.

[4] Richard B. Larson. The evolution of molecular clouds. *Yale Department of Astronomy*.

[5] John S. Mathis, Barbara A. Whitney, and Kenneth Wood. Can reflection from grains diagnose the albedo? *The Astrophysical Journal*, 574(2):812–821, August 2002.

[6] Joseph C. Watkins. An introduction to the science of statistics: The law of large numbers. http://math.arizona.edu/~jwatkins/statbook.pdf.